Nanoscale

Accepted Manuscript

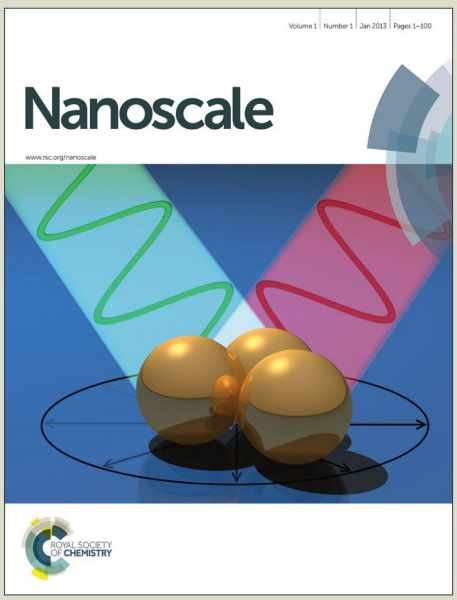

ROYAL SOCIETY OF CHEMISTRY

www.rsc.org/nanoscale

Highly Efficient and Durable TiN Nanofiber Electrocatalyst Supports

Hyun Kim[1,2], Min Kyung Cho[3], Jeong An Kwon[4], Yeon Hun Jung[1], Kyung Jin Lee[1], Na Young Kim[1], Min Jung Kim[5], Sung Jong Yoo[1], Jong Hyun Jang[1,2], Hyoung-Juhn Kim[1], Suk Woo Nam[1,2], Dong-Hee Lim[4], EunAe Cho[5,], Kwan-Young Lee[2,*], and Jin Young Kim[1,*]*

[1]Fuel Cell Research Center, Korea Institute of Science and Technology, Seongbuk-Gu, Seoul 136-791, Republic of Korea

[2]Green School, Korea University, 145, Anam-ro, Seongbuk-gu, Seoul 136-701, Republic of Korea

[3]Advanced Analysis Center, Korea Institute of Science and Technology, Seongbuk-Gu, Seoul 136-791, Republic of Korea

[4]Department of Environmental Engineering, Chungbuk National University, Chungdae-ro 1, Seowon-gu, Cheongju, Chungbuk 362-763, Republic of Korea

[5]Department of Materials Science and Engineering, Korea Advanced Institute of Science and Technology, Daejeon, Republic of Korea

[*]Corresponding authors:

EunAe Cho; eacho@kaist.ac.kr, Kwan-Young Lee; kylee@korea.ac.kr, Jin Young Kim; jinykim@kist.re.kr

Abstract

To date, carbon-based materials including various carbon nanostructured materials, have been extensively used as electrocatalyst support for proton exchange membrane fuel cell (PEMFC) applications due to its practical nature. However, carbon dissolution or corrosion caused by high electrode potential in the presence of O_2 and/or water has been identified as one of the main failure modes for the device operation. Here, we report the first TiN nanofibers (TNFs)-based nonwoven structured materials to be constructed via electrospinning and subsequent two-step thermal treatment processes as a support for the PEMFC catalyst. Pt catalyst nanoparticles (NPs) deposited on the TNFs (Pt/TNFs) were electrochemically characterized with respect to oxygen reduction reaction (ORR) activity and durability in an acidic medium. From the electrochemical tests, the TNFs-supported Pt catalyst was better and more stable in terms of its catalytic performance compared to a commercially available carbon-supported Pt catalyst. For example, the initial oxygen reduction performance was comparable for both cases, while Pt/TNF showed much higher durability from accelerated degradation test (ADT) configuration. It is understood that the improved catalytic roles of TNFs on supported Pt NPs for ORR are due to the high electrical conductivity arising from the extended connectivity, high inertness to the electrochemical environment and strong catalyst-support interactions.

As a catalyst support for proton exchange membrane fuel cell (PEMFC) applications, nanostructured carbon materials have been generally used due to their large surface area and high electrical conductivity.[1-3] However, the carbon-based materials are often susceptible to corrosive conditions in a wide range of fuel cell operation modes. In particular, it has been documented that carbon corrosion can be initiated at high water content, low pH (<1), high temperature (50-90°C), high oxidative potential (0.6-1.2 V), and high oxygen concentration.[4,5] Subsequent carbon oxidation to CO_2 on the surface has been observed, leading to the degradation of output performance of the cell.[6]

To address these issues, there has been a growing interest in recent years to develop alternative non-carbon support materials for the manufacture of fuel cell devices in order to improve their durability, while simultaneously maintaining the catalysts activity.[7-10] However, there have, as of yet, been limited strategies to prepare nanostructured supports on a facile and scalable pathway to meet the both purposes.

In this study, we have investigated titanium nitride nanofibers (TNFs) as a catalyst support for PEMFCs. The titanium nitride (TiN) can be potentially useful as a candidate for the highly durable catalysts support with its stability in fuel cell operation atmosphere due to its high resistance to electrochemical corrosion and high electrical conductivity.[11-15] However, few strategies exist to prepare nanostructured nitrides on a scalable and inexpensive pathway.[16]

Here, we present the 3-dimensionally interconnected TNFs assemblies synthesized by a combination of electrospinning and two-step calcination techniques. They exhibited high electrical conductivity and accelerated the electron transfer, as verified by four-point probe method and cyclic voltammetry (CV). CV and rotating disk electrode (RDE) test results showed that the TNF-supported Pt catalysts (Pt/TNFs) showed much more prominent electrocatalytic stabilities than carbon-supported ones, while yielding similar initial oxygen reduction activity. The improvement of electrocatalytic activity and durability has been presumably originated from the high electrical conductivity, high chemical inertness of TNF and a strong interaction with Pt.

We synthesized TNFs by electrospinning of titanium sol-gel precursor titanium tetraisopropoxide ($Ti(O^iPr)_4$)/polyvinylpyrrolidone (PVP) mixture solution followed by two-

step thermal treatment processes for the nitridation (Fig. 1a and Fig. S1). First, we dissolved $Ti(O^iPr)_4$ and PVP in a mixture of ethyl alcohol and acetic acid and then electrospun the solution onto a grounded electrode. PVP was selected as the polymer precursor of electrospun nanofibers, because it has been widely used as a precursor for polymeric nanofibers and it is soluble in various organic solvents.

The conversion of the prepared Ti-containing polymeric nanofibers to TiN was performed in a two-step post-heat treatment processes, which involved stabilization and nitridation processes. They were first heat-treated at 700°C for 1h in air to convert into TiO_2 arising from thermal decomposition of the polymeric phase. Then, the oxide compounds were transformed into nitride through the second calcination step above 900°C under NH_3.[17,18]

X-ray diffraction (XRD) patterns obtained after the thermal treatment processes of electrospun fibers are presented in Fig. 1b. In the first stage of thermal treatment process, amorphous polymeric nanofiber was transformed through TiO_2 form. Then, TiO_2 nanofibers were converted to TNFs when annealed at high temperature in NH_3. Importantly, the phase transformation into nitride took place above 900°C. The major peaks of produced TNFs located at $2\theta = 36.9°$ and 42.8° were indexed as (111) and (200) planes, respectively. They were the characteristics for the pure phase cubic TiN crystallites. It is noted that the sharp peaks indicated that the products synthesized in this study were highly crystalline materials. Further, the prepared TNFs exhibited very low electrical resistance of ~0.65 ohm $square^{-1}$ from four-point probe method (Table S1).

Scanning electron microscopy (SEM) image shows that the as-prepared TNFs have a diameter ranging from 100 to 200 nm with tens of micrometers in length depending on applied voltage and tip diameter (Fig. 1c and Fig. S2). The detailed morphologies and the size of as-prepared TNFs were further characterized by transmission electron microscopy (TEM), indicating that the surface of nanofibers became rough and grainy (Fig. S3). Furthermore, these results revealed that one-dimensional TNFs formed three-dimensional network structure, which were beneficial to large electrode surface and facile electron transport for catalytic application.

The surface area and pore size distribution of the prepared TNF samples were examined using nitrogen adsorption/desorption isotherms (Fig. S4). There are more

micropores with radii of less than 3 nm in the Pt/TNF. The specific surface area and the micropore volume of prepared TNFs are summarized in Table S2. The optimum sample of prepared TNF (diameter ≈ 100 nm) had a surface area of 181 m^2 g^{-1}.

We then sought to prepare Pt catalysts on the produced TNFs to investigate the electrocatalyst's performance. Electrospun nanofibers have proven to be efficient three-dimensional scaffold to generate catalytic particles owing to the high porosity and large surface areas. Several NP synthetic methods were applied for the preparation of nanosized Pt catalysts on the electrospun TNFs and a polyol reduction method was optimal for our synthetic condition (Fig. S5).[19,20]

Figure 2 shows a high-resolution TEM (HRTEM) image of Pt/TNF structures. A uniform distribution and absence of agglomeration of Pt NPs are observed throughout the entire TNF support surface. The formation of essentially monodisperse and highly dispersed Pt particles is ascribed to the protecting role of PVP at the surface of the nascent NPs in the NP synthetic process. Pt NPs follow the ups and downs along the TNF surface, forming a 3D nano-architectured catalyst layer. All of the Pt NPs were projected randomly outwards from the support surface. They had a small diameter of 2.5-7 nm, with a lattice fringe spacing of 0.23 nm, which corresponded to the interplanar separation of {111} planes of the bulk Pt crystal. It has been reported that for Pt NPs synthesized by chemical reduction method, all of three low-index facets of {100}, {110}, and {111} are mainly exposed.

The Pt loading on the prepared Pt/TNFs was controlled to 20 wt% measured by inductively coupled plasma mass spectrometry measurement (Note that the same weight percentage of the commercial Pt/C catalyst was compared in the study). Elemental mapping of Pt/TNFs was conducted to verify the elemental composition of the nanofibers. Ti, N and Pt atoms were confirmed and well distributed on the nanofiber matrix. TEM energy-dispersive X-ray analysis (EDS) scan profile indicated the uniform distribution of Pt, Ti and N components in a representative single nanofiber (Fig. 3).

We then turned to examine the electrochemical properties of Pt/TNFs (Fig. 4). A commercial Pt/C catalyst with the same weight of Pt percentage (Tanaka, 20 wt%) was compared simultaneously using the same procedure. The catalytic activities of Pt/TNFs structures were obtained on a rotating disk electrode (RDE) in an O_2-saturated 0.1 M $HClO_4$

solution at 1,600 rpm. As shown in Fig. 4a and 4b, Pt/TNF and Pt/C exhibited similar ORR initial activities with half-wave potentials of ~0.88 V.

The durability of catalysts was evaluated using the accelerated degradation test (ADT) by potential cycling between 0.6 and 1.1 V for 6,000 cycles in air-saturated 0.1 M $HClO_4$ solution at a scan rate of 5 mV s^{-1}. Figure 4 shows the excellent cyclic stability of Pt/TNFs, indicating the superior stability compared to the Pt/C reference. Moreover, the degradation of the electrochemical surface area of Pt NPs is greatly suppressed when Pt is supported on TNFs as compared with that on carbon black, which corresponds to particle size change of Pt catalysts by TEM analysis, as shown in Fig. 5. The structural stability of TNFs after the electrochemical cycling was further verified by annular dark field scanning TEM (ADF-STEM) images and electron energy-loss spectroscopy (EELS) elemental mapping, as shown in Fig. S6-S7, indicating that TNF is essentially stable under the ORR conditions.

It is generally known that the electrochemical surface area of Pt is one of the most important factors that influences the performance of a fuel cell electrode.[21] To get a better insight for the decreased Pt particle size change on TNFs, the interaction between Pt and support was analyzed by X-ray photoelectron spectroscopy (XPS) (Fig. 6). The XPS results showed that the peak maximum of Pt/TNF shifted to higher binding energy (74.2 eV) with respect to Pt/C (71.8 eV). The strong interaction between Pt and TNF was evidenced to have the higher binding energy compared to that of the Pt/C catalysts. Generally, strong interaction has a major positive effect on the enhanced catalytic activity and the improvement of the catalyst durability.[22,23]

Density functional theory (DFT) calculations have also shown that the interaction between Pt and TiN is stronger than that of Pt and carbon. The adsorption energies (E_{ads}) of Pt_6 cluster were -6.91 eV at a hollow site of TiN(100) and -0.82eV at a bridge site of graphene. The more negative E_{ads} represents the stronger binding of Pt_6 on the surface. The stronger binding of Pt_6 on TiN(100) is attributed to the stronger interaction between Pt and Ti rather than Pt and N on the surface. As Pt_6 adsorbs on TiN, Pt_6 is strongly distorted due to the significant interaction between Pt and Ti. On the other hand, graphene without any defects, shows weak interaction toward Pt. Details are described in Supplementary Information, Fig. S8, and Table S3.

Conclusions

TNF network structured materials can be a promising alternative for PEMFC electrocatalyst supports, with the advantage of a simple and easily up-scalable preparation method. Herein, for the first time this study reports the applicability of electrospun TNFs structures. We fabricated TNFs by the combination of a simple electrospinning and subsequent thermal treatment processes, and then decorated their surfaces with Pt NPs of 2.5-7 nm in diameter. Such Pt/TNFs exhibited comparable electrocatalytic activity in comparison with commercial Pt/C. Furthermore, the novel Pt/TNF materials demonstrated high electrochemical stability after accelerated stress tests. The dramatically enhanced corrosion resistance of TNF-based support is ascribed to the extended connectivity and high chemical and electrochemical stability compared to carbon.

Acknowledgements

This study was supported by the Korean Government through the New and Renewable Energy Core Technology Program of the Korea Institute of Energy Technology Evaluation and Planning (KETEP) funded by MOTIE (No.20133030011320), (No.20143030031340), the Korea CCS R&D Center (KCRC) grant funded by MSIP (No. 2015M1A8A1049349), the National Research Foundation of Korea Grant funded by MSIP (2015, University-Institute cooperation program), and the Global Frontier R&D Program at the Center for Multiscale Energy System funded by the National Research Foundation, MSIP (No. 2012M3A6A7054283). This work was also financially supported by KIST through Institutional Project (2E25411). The current work is supported by Basic Science Research Program through the National Research Foundation (NRF) of Korea funded by the Ministry of Education, Science and Technology (NRF-2012R1A6A3A04040490).

Competing Financial Interests

The authors declare no competing financial interests.

References

1. J. P. Meyers and R. M. Darling, *J. Electrochem. Soc.*, 2006, **153**, A1432-A1442.
2. E. Auer, A. Freund, J. Pietsch and T. Tacke, *Appl. Catal. A*, 1998, **173**, 259-271.
3. T. Ralph and M. Hogarth, *Platin. Met. Rev.*, 2002, **46**, 117-135.
4. L. Roen, C. Paik and T. Jarvi, *Electrochem. Solid-State Lett.*, 2004, **7**, A19-A22.
5. W. R. Baumgartner, E. Wallnofer, T. Schaffer, V. Hacker, V. Peinecke and P. Prenninger, *ECS Trans.*, 2006, **3**, 811-825.
6. X. Yu and S. Ye, *J. Power Sources*, 2007, **172**, 145-154.
7. M. Yang, A. R. V. Wassen, R. Guarecuco, H. D. Abruna and F. J. DiSalvo, *Chem. Commun.*, 2013, **49**, 10853-10855.
8. H. Lv and S. Mu, *Nanoscale*, 2014, **6**, 5063-5074.
9. S. Sharma and B. G. Pollet, *J. Power Sources*, 2012, **208**, 96-119.
10. Y. J. Wang, D. P. Wilkinson and J. Zhang, *Chem. Rev.*, 2011, **111**, 7625-7651.
11. K. Kakinuma, Y. Wakasugi, M. Uchida, T. Kamino, H. Uchida, S. Deki and M. Watanabe, *Electrochim. Acta*, 2012, **77**, 279-284.
12. M. Yang, Z. Cui and F. J. DiSalvo, *Phys. Chem. Chem. Phys.*, 2013, **15**, 1088-1092.
13. M. O. Thotiyl, T. R. Kumar and S. Sampath, *J. Phys. Chem. C*, 2010, **114**, 17934-17941.
14. R. Kumar, S. Pasupathi, B. G. Pollet and K. Scott, *Electrochim. Acta*, 2013, **109**, 365-369.
15. Y. Xiao, G Zhan, Z. Fu, Z. Pan, C. Xiao, S. Wu, C. Chen, G. Hu and Z. Wei, *Electrochim. Acta*, 2014, **141**, 279-285.
16. Y. Xia, P. Yang, Y. Sun, Y. Wu, B. Mayers, B. Gates, Y. Yin, F. Kim and H. Yan, *Adv. Mater.*, 2003, **15**, 353-389.
17. M. Zukalova, J. Prochazka, Z. Bastl, J. Duchoslav, L. Rubacek, D. Havlicek and L. Kavan, *Chem. Mater.*, 2010, **22**, 4045-4055.
18. D. Sun, J. Lang, X. Yan, L. Hu and Q. Xue, *J. Solid State Chem.*, 2011, **184**, 1333-1338.
19. H. S. Oh, J. G. Oh and H. Kim, *J. Power Sources*, 2008, **183**, 600-603.
20. K. Lee, J. Zhang, H. Wang and D. P. Wilkinson, *J. Appl. Electrochem.*, 2006, **36**, 507-522.
21. W. Schmittinger and A. Vahidi, *J. Power Sources*, 2008, **180**, 1-14.
22. X. Yu and S. Ye, *J. Power Sources*, 2007, **172**, 133-144.
23. Y. Shao, G. Yin and Y. Gao, *J. Power Sources*, 2007, **171**, 558-566.

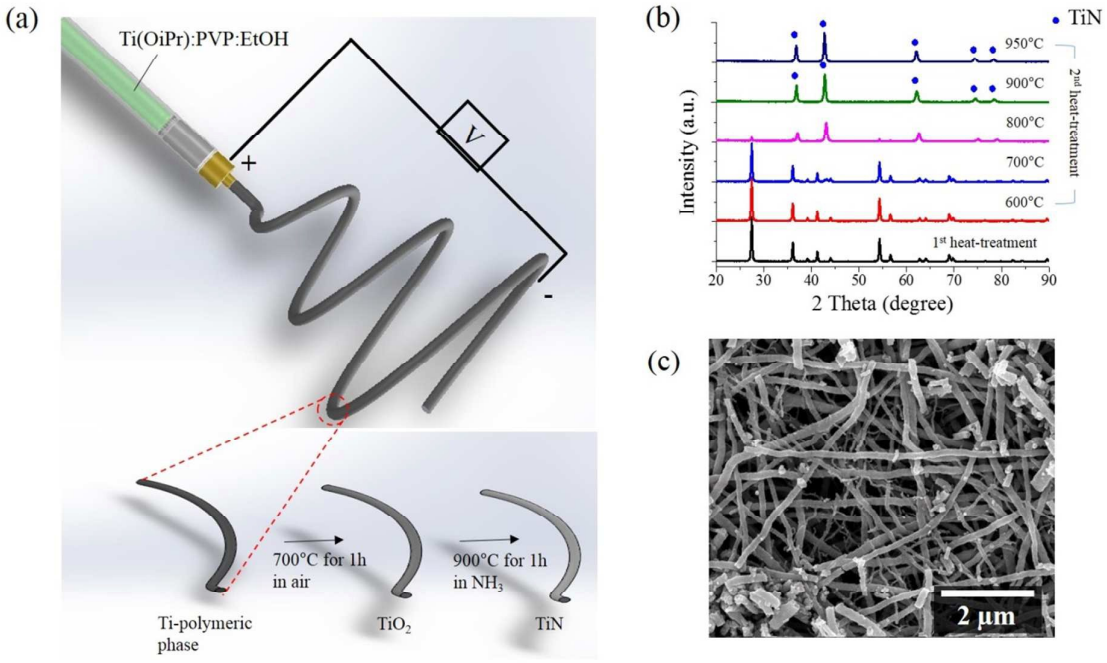

Figure 1. (a) Schematic depiction of TNF synthesis via electrospinning, followed by two-step subsequent thermal treatment. (b) XRD patterns of Ti(OiPr)/PVP nanofibers after first heat-treatment and after second heat-treatment carried out at different temperatures in NH_3 atmosphere. (c) SEM image of the prepared TNF.

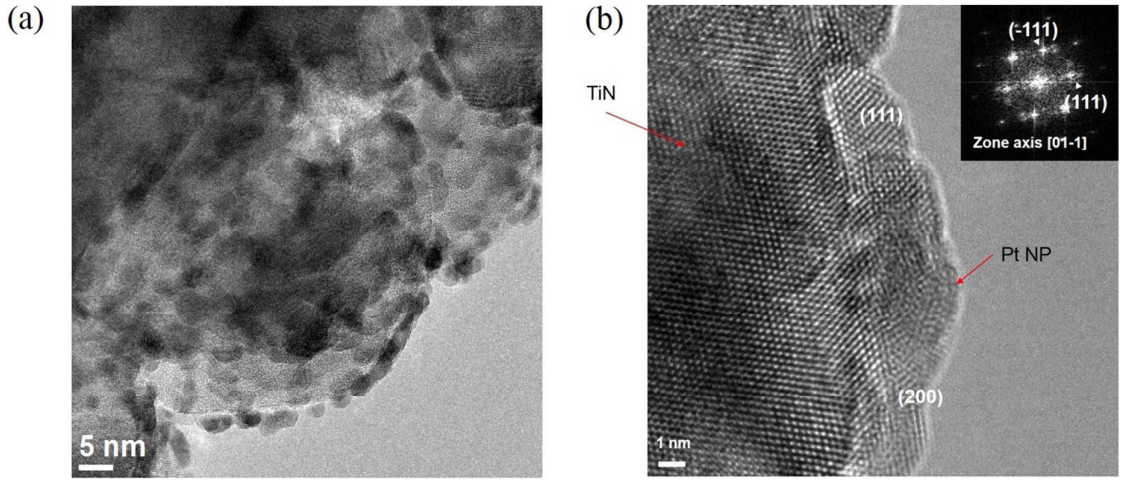

Figure 2. (a) TEM image of Pt NPs loaded on TNF. (b) HRTEM image of Pt/TNF. The inset shows the diffraction pattern of the selected area of Pt/TNF, which indicates the diffraction from crystalline planes of Pt NPs corresponding to {111} planes.

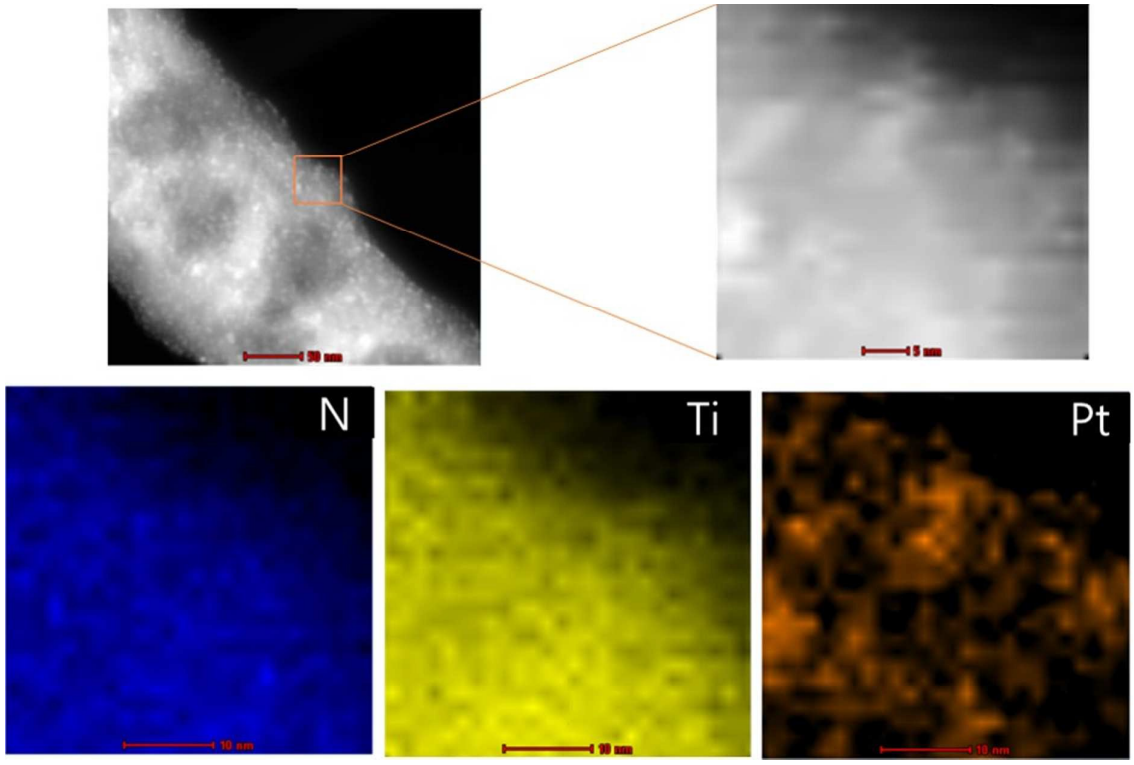

Figure 3. STEM-HAADF image and EDS elemental maps showing the spatial distribution of N, Ti, and Pt on Pt/TNF.

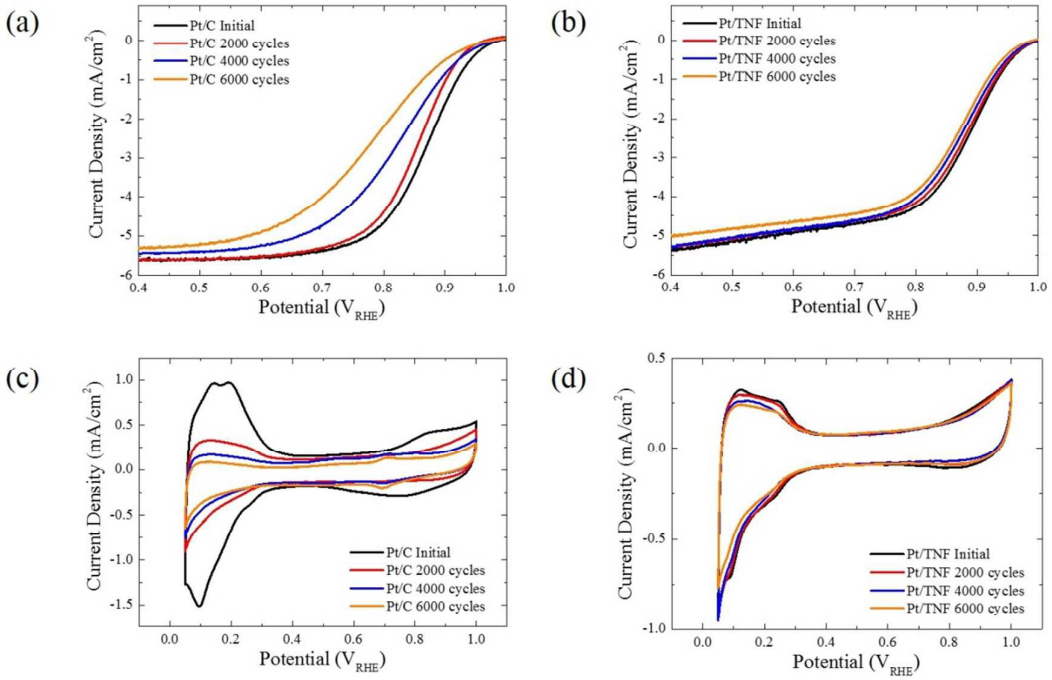

Figure 4. ORR Polarization curves of (a) Pt/C and (b) Pt/TNF catalysts obtained before and after ADT experiment. CV curves of (c) Pt/C and (d) Pt/TNF catalysts obtained before and after ADT experiment. The ADT experiment was carried out in air-saturated 0.1 M $HClO_4$ solution with the cyclic potential sweeping between 0.6 and 1.1 V at a scan rate of 5 mV s^{-1}.

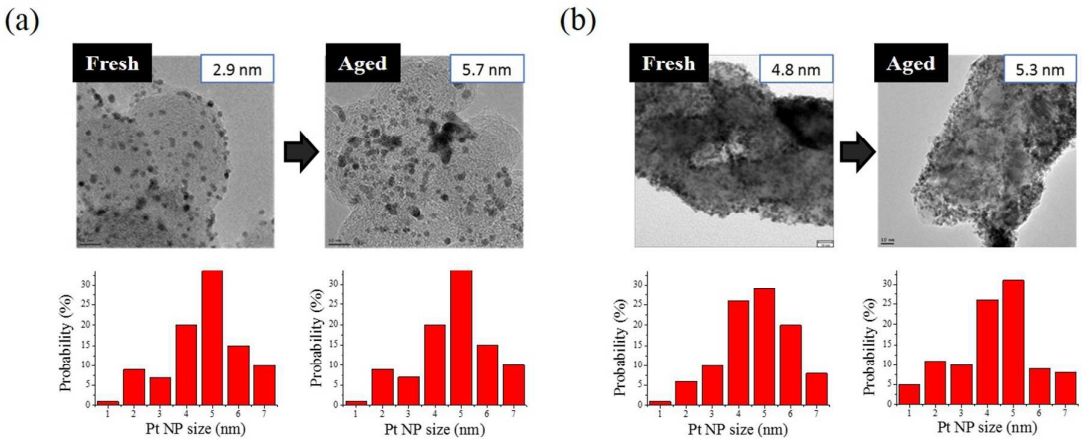

Figure 5. TEM images and Pt NP size histograms of (a) Pt/C and (b) Pt/TNF electrocatalysts obtained before and after the ADT test.

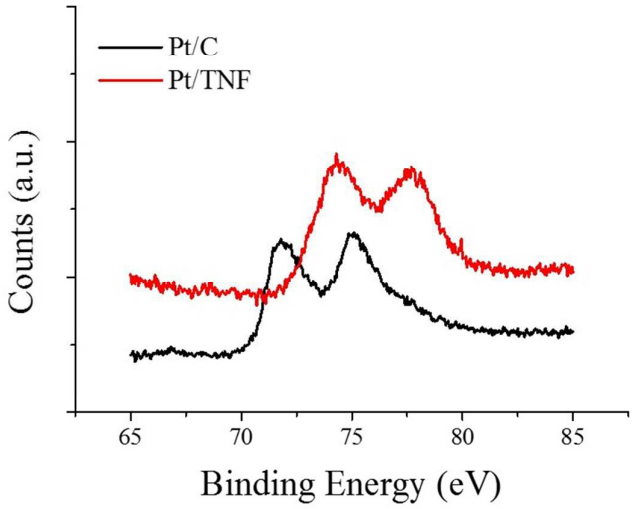

Figure 6. Pt 4f XPS spectra of Pt/TNF and Pt/C catalysts.